# Environmental Science
## Processes & Impacts

Accepted Manuscript






ROYAL SOCIETY OF CHEMISTRY

rsc.li/process-impacts

## Table of contents entry

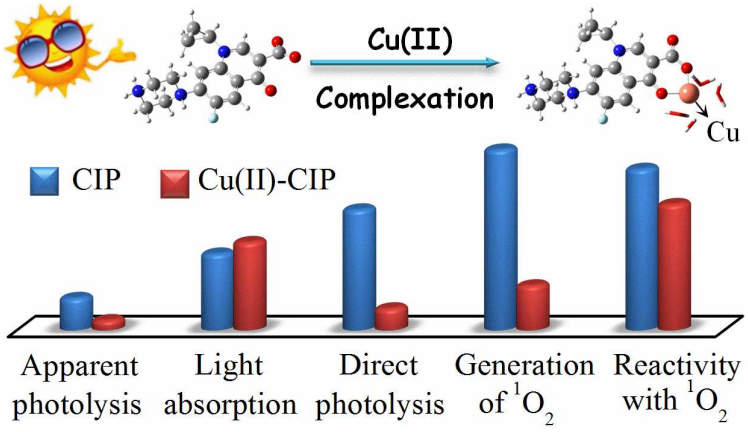


Cu(II) complexation altered the light absorption, direct photolytic pathways, $^1O_2$ photo-generation ability, and the reactivity of $H_2CIP^+$ towards $^1O_2$ by changing its molecular orbitals and atomic charge distribution.

## Environmental impact

To support 10 billion people in 2050, aquaculture and livestock breeding could be an important strategy. To ensure the production, thousands of tons of antibiotics and metal trace elements are used as feed additives per year and their combined pollution becomes more and more prominent. The interaction between them may affect the environmental behavior and ecotoxicology of antibiotics, and increase the uncertainty of risk assessment. As many antibiotics are resistant to microbial-degradation, photodegradation becomes pivotal in determining their fate and ecological risk. Here we proved that metal can complex with antibiotics, and then alter their photolytic reactivity and pathways. Additionally, we enlighten a computational approach to predict the photochemical behavior for antibiotics in different aqueous forms and clarify the photolytic mechanisms.

# Photochemical Behavior of Antibiotics Impacted by Complexation Effects of Concomitant Metals: A Case for Ciprofloxacin and Cu(II)[†]

Xiaoxuan Wei,[a] Jingwen Chen,[*a] Qing Xie,[a] Siyu Zhang,[ab] Yingjie Li,[a] Yifei Zhang,[a] and Hongbin Xie[a]

[a] Key Laboratory of Industrial Ecology and Environmental Engineering (MOE), School of Environmental Science and Technology, Dalian University of Technology, Dalian 116024, China

[b] Key Laboratory of Pollution Ecology and Environmental Engineering, Institute of Applied Ecology, Chinese Academy of Science, Shenyang 110016, China

## Abstract

Many water bodies, especially those adjacent to aquaculture and livestock breeding areas, are contaminated by both antibiotics and transition metals. However, the effects of the interaction between antibiotics and transition metals on the environmental behavior and the ecotoxicology of antibiotics are largely unknown. We hypothesized that antibiotics may coordinately bind with metal ions, and this complexation may affect the environmental photochemical behavior of antibiotics. We took ciprofloxacin (CIP) and Cu(II) as a case, and employed simulated sunlight experiments and density functional theory calculations to investigate the underlying reaction mechanisms. Results showed that monovalent cationic ciprofloxacin ($H_2CIP^+$) that is predominant in the normal pH range (6~9) of surface waters,

[†] Electronic Supplementary Information (ESI) available: details of the total ion chromatograms and mass spectra of the identified products, the product yields, and the formation and degradation rate constants.

[*] Correspondence to: Jingwen Chen, e-mail: jwchen@dlut.edu.cn; Phone: +86-411-8470 6269

[a] Dalian University of Technology

[b] Institute of Applied Ecology, Chinese Academy of Science

can chelate with hydrated Cu(II) to form $[Cu(H_2CIP)(H_2O)_4]^{3+}$. Compared with $H_2CIP^+$, $[Cu(H_2CIP)(H_2O)_4]^{3+}$ has different molecular orbitals, and atomic charge distribution. As a result, $[Cu(H_2CIP)(H_2O)_4]^{3+}$ showed dissimilar light absorption properties, slower direct photolytic rates, lower $^1O_2$ generation ability and weaker reactivity towards $^1O_2$. Due to the Cu(II) complexation, the apparent photodegradation of $H_2CIP^+$ was inhibited, and the photolytic pathways and product distribution were altered. This study implies that for accurate ecological risk assessment of antibiotics under transition metal co-contamination conditions, the effects of metal complexation should be considered.

**Keywords:** Photochemical behavior, Antibiotics, Metal complexation

## Introduction

Antibiotics are of acute concern as they are pseudo-persistent in the aquatic environment[1] and many of them can induce bacterial resistance even at environmental concentrations.[2] In recent years, the combined pollution of antibiotics and transition metals (Cu, Zn, Fe, etc.) became evident, especially in natural waters adjacent to aquaculture and livestock breeding areas where both trace elements and antibiotics are used as feed additives.[3,4] For example, the concentrations of some antibiotics and transition metals were up to 6.8 and 55.0 μg/L, respectively, in coastal waters of the China Bohai bay due to marine aquaculture.[5,6] The molecular structures of most antibiotics, such as fluoroquinolones and tetracyclines, contain heteroatoms (e.g., O and N). Theoretically, these antibiotics can coordinately bind with metal ions, leading to the formation of metal complexes.[7,8] The complexation may alter the physicochemical properties (e.g., octanol-water partition coefficient) and chemical reactivity of antibiotics.[9,10] As a result, the environmental fate and ecotoxicology of antibiotics are altered.[11–13] Thus, it is of importance to explore the effects of complexation on the environmental behavior and ecotoxicology of antibiotics, for the purpose of ecological risk assessment of antibiotics under the combined pollution with transition metals.

Photochemical degradation has been proven to be a central factor in determining the environmental fate of most antibiotics.[14,15] In addition to direct photodegradation, some antibiotics, such as fluoroquinolones and tetracyclines, can also photo-generate reactive oxygen species (ROS, e.g., singlet oxygen $^1O_2$ and hydroxyl radical ·OH), and be oxidized by ROS produced by themselves (i.e. self-sensitized photooxidation) or by other water constituents.[16-18] Some previous studies have observed that metal ions could affect the photolytic kinetics of antibiotics. For example, the photolytic rate constants ($k$) of tetracycline at varied Mg(II) and Ca(II) concentrations relevant to the natural conditions were found to vary by up to one order of magnitude.[11] Clarithomycin and roxithromycin cannot directly photodegrade in environmental waters as they do not absorb sunlight ($\lambda$ > 290 nm), nevertheless their Fe(III)-complexes undergo direct photolysis in sunlit waters.[19]

The mechanisms underlying the impact of metal complexation on the photodegradation of antibiotics and other trace organic pollutants are largely unknown. We hypothesized that metal complexation can have effects on the photochemical reactivity of antibiotics through the following four ways: (1) As new chemical bonds are formed by complexation, the formed metal complexes may have different light absorption characteristics; (2) The formed metal complexes may have direct photolytic pathways that are different from the pathways of the corresponding antibiotics; (3) The complexes and the corresponding antibiotics may have different ROS generation abilities; and (4) The complexes and the corresponding antibiotics may have different reactivity towards ROS.

In this study, we adopted ciprofloxacin (CIP, a widely used fluoroquinolone) and Cu(II) (a common transition metal with strong complexing ability) as a case to verify the hypothesis. In the normal pH range (6~9) of surface waters, monovalent cationic ciprofloxacin ($H_2CIP^+$) is the predominant dissociation species of CIP.[20] It can undergo both direct photolysis and self-sensitized photooxidation via ROS (e.g., $^1O_2$). Previous studies have observed that metals,

e.g. Cu(II), Zn(II), Fe(III), can affect the photodegradation of fluoroquinolones.[21,22] However, the underlying mechanisms are not clear and need clarification.

We employed fluorescence spectrophotometric titration and infrared spectrometry to examine the complexation between CIP and Cu(II). Simulated sunlight experiments were performed to explore the effects of Cu(II) complexation on the photochemical behavior of CIP. In addition, density functional theory (DFT) calculations were performed to provide complementary insights into the impact of Cu(II) complexation on the photolysis of CIP.

## Materials and methods

### Chemicals and Reagents

Ciprofloxacin (CIP) with 98.0% purity was provided by Zhejiang Guobang Pharmaceutical Co., Ltd. Deuterium oxide ($D_2O$, 99.9%) and perinaphthenone (97% purity) were obtained from Sigma-Aldrich. Furfuryl alcohol (FFA, 90% purity) was purchased from Shanghai Jinshan Ting New Chemical Reagent Factory. Acetonitrile and trifluoroacetic acid were of HPLC grade and purchased from Tedia Inc. Other reagents (purity > 99.0%) were purchased from Kermel Chemical Reagent Co., Ltd. Ultrapure water (18 MΩ cm) was obtained from an OKP ultrapure water system produced by Shanghai Lakecore Instrument Co., Ltd.

### Characterization of the Complex

The complexation of CIP with Cu(II) in pH = 7.5 solutions was verified by a fluorescence spectrophotometric titration technique. Fluorescence spectra were recorded using a Hitachi F-4500 fluorescence spectrometer. Fluorescence intensity of the solutions at Ex/Em = 280/430 nm was used to calculate the complex ratio and the conditional stability constant ($K'_f$) on the basis of the Lineweaver-Burk equation[13] (detailed in Text S1 of the Electronic Supplementary Information, ESI).

To identify the complexation sites, the Cu(II)-CIP complex was prepared according to the procedures reported by Zhang et al.[13] (Text S2). IR spectra from 1% solid dispersions in KBr

were recorded by Fourier transform infrared spectroscopy (IR-Prestige-21, Shimadzu, Japan).

**Photodegradation Experiments**

The photolytic experiments were performed with an XPA-7 merry-go-round photoreactor (Xujiang Electromechanical Plant, China). A water-refrigerated 1000 W xenon lamp surrounded by Pyrex filters was used to simulate the sunlight with $\lambda > 290$ nm. The irradiance measured by a UV-365 radiometer (Photoelectric Instrument Factory of Beijing Normal University, China) was 294 μW/cm$^2$ in the center of the tubes. All the CIP solutions (5 μmol/L) were adjusted to pH = 7.5 with HCl/NaOH only, so as to avoid the possible effects of buffers.[23] pH values were measured with a Mettler Toledo S40-K pH-meter equipped with an InLab®Expert Pro combined electrode. The pH values changed slightly (< 0.5 pH units) during the photolytic experiments. The ionic strength was controlled with NaCl (1 mmol/L). UV-vis absorption spectra of CIP (5 μmol/L) were recorded via a Hitachi U-2900 spectrophotometer using a 1 cm cuvette. As the absorbance in the effective wavelength range (290~400 nm) is > 0.02, all the observed photolytic rate constants were corrected for light-screening.[20]

Ethylene diamine tetraacetic acid (EDTA), a typical complexing agent (conditional stability constant $K'_{f,Cu(EDTA)} = 1.0 \times 10^{16}$ L/mol, pH = 7.5),[24] was employed to assess the role of Cu(II) complexation on the photodegradation of CIP. The direct photodegradation of CIP was investigated in $N_2$ saturated solutions. To examine the $^1O_2$ generating ability of CIP irradiated by simulated sunlight, FFA was used as a probe compound, and $D_2O$ was employed to prolong the lifetime of $^1O_2$.[25] The steady-state concentration of $^1O_2$ was calculated as follows:

$$[^1O_2] = \frac{k_{FFA}}{k_{1O2,FFA}} \quad (1)$$

where $k_{FFA}$ is the observed degradation rate constant for FFA, $k_{1O2,FFA}$ is the known reaction rate constant for FFA with $^1O_2$ ($k_{1O2,FFA} = 8.3 \times 10^7$ L mol$^{-1}$s$^{-1}$ in $D_2O$),[26] and $[FFA]_0$ = 10 μmol/L. The reactivity of CIP towards $^1O_2$ was assessed by a second-order reaction rate

constant, $k_{1O2}$. For the determination of $k_{1O2}$, perinaphthenone was used as the $^1O_2$ photosensitizer, and FFA as a reference compound ($k_{1O2,FFA}$ = 1.2 × $10^8$ L $mol^{-1}s^{-1}$ in $H_2O$).[27] The initial concentrations of perinaphthenone, FFA and CIP were 20 μmol/L and the concentration of Cu(II) was 40 μmol/L. A 300 W Hg lamp surrounded by 380 nm cut-off filters was employed as the light source, under which the direct photodegradation of CIP and FFA can be neglected, and CIP cannot photogenerate $^1O_2$ as these compounds have no light absorption at these conditions. The $k_{1O2}$ value of CIP was calculated with the following equation:

$$k_{1O2,CIP} = \frac{\ln([CIP]_t / [CIP]_0)}{\ln([FFA]_t / [FFA]_0)} k_{1O2,FFA} \quad (2)$$

**Analytical Determinations**

The concentration of CIP was determined by an Agilent 1100 HPLC with a ZORBAX SB-C18 column (2.1 mm × 150 mm, 3.5 μm). CIP was excited at $\lambda$ = 280 nm and recorded at $\lambda$ = 445 nm with a fluorescence detector. The mobile phases were acetonitrile (A) and trifluoroacetic acid in water (pH = 2.4) with the following gradient elution: 5% A (0 min) to 20% A (3 min) to 40% A (15 min) to 5% A (17−20 min). For FFA, the detection wavelength was 230 nm with a diode array detector, and the mobile phase was made up of 10% acetonitrile and 90% $H_2O$. The flow rate was 0.2 mL/min, injection volume was 5 μL, and column temperature was 30 °C.

Photolytic products were separated by an Agilent 1200 HPLC. The gradient eluting condition of HPLC was: 2% A (0 min) to 12% A (3 min) to 20% A (28 min) to 38% A (43 min) to 2% A (44−50 min). The other separation conditions were the same as in case of the analytical method of CIP. The accurate masses of the products were determined by an Agilent 6224 TOF mass spectrometer, and the mass spectral fragmentation patterns were examined by an Agilent 6410B triple quadrupole mass spectrometer. The mass spectrometer conditions were: ionization mode: ESI, positive mode; scan range: *m*/*z* 50−1000; drying gas flow: 9

L/min; drying gas temperature: 350 °C; fragmentor: 150 V; nebulizer pressure: 40 psi; capillary voltage: 4000 V; skimmer voltage: 65 V; octapole radio frequency voltage: 750 V.

**DFT Computation**

All the calculations were performed with the Gaussian 09 program suite,[28] using the M06-2X hybrid meta exchange-correlation functional[29] with the 6-31+G(d,p) basis set for C, N, O, F, H, and the LanL2DZ pseudopotential[30] and the basis set for Cu. The solvent effect of water was considered by the integral equation formalism of the polarized continuum model (IEFPCM) based on the self-consistent-reaction-field (SCRF) method.[31] The possible defluorination reactions were calculated for $H_2CIP^+$ (the dominant dissociation species of CIP in pH = 7.5 solution) at the lowest excited triplet state (T),[32,33] and for its Cu(II) complex at the excited tripquartet state ($^4$T, where the quartet superscript refers to the total spin of the complex, T refers to the local multiplicity of $H_2CIP^+$).[34,35] The excited-state geometries of $H_2CIP^+$ and its Cu(II) complex were calculated by adjusting the spin multiplicity to 3 and 4, respectively.[36,37] Frequency calculations were performed to determine the character of stationary points. Transition states (TS) were characterized with only one imaginary vibrational frequency. Intrinsic reaction coordinate (IRC) analysis[38] was executed to verify that each TS uniquely connected the designated reactants with the products. Values of the Gibbs free energy and the enthalpy were corrected by thermal energy at 298 K. Atomic charges were evaluated by Mulliken charge analysis.[39]

## Results and discussion

**Complexation between Ciprofloxacin and Cu(II)**

The fluorescence spectrophotometric titration results (Fig. S1) show that Cu(II) and CIP can form a 1:1 complex with a conditional stability constant $K'_{f,Cu(CIP)} = 1.23 \times 10^6$ L/mol in pH = 7.5 solutions. As shown in Equation (3), the fraction of Cu(CIP) ($\alpha_{Cu(CIP)}$) depends only on the equilibrium concentration of the free Cu(II) ion ([$Cu^{2+}$]). According to the previous studies of

Cu(II) speciation in natural waters, $[Cu^{2+}]$ is in the range of $10^{-6}$~$10^{-16}$ mol/L at the complexation equilibrium with organic matters.[40–42] When $[Cu^{2+}]$ = 1 μmol/L, $\alpha_{Cu(CIP)}$ is about 55% (Fig. S2). These findings indicate that Cu(II) can significantly affect the chemical speciation of CIP in some water bodies.

$$\alpha_{Cu(CIP)} = \frac{[Cu(CIP)]}{[CIP]+[Cu(CIP)]} = \frac{K'_{f,Cu(CIP)}[Cu^{2+}]}{1+K'_{f,Cu(CIP)}[Cu^{2+}]} \quad (3)$$

We observed pronounced differences in IR spectra for CIP alone and CIP with the coexistence of Cu(II) (Fig. S3). From the IR spectrum of CIP and the spectrum of the Cu(II)-CIP complex, the C=O stretching vibration of the carboxyl group (~1710 $cm^{-1}$) disappeared, and a shift to low wavenumbers (from 1610 $cm^{-1}$ to 1585 $cm^{-1}$) was observed in the carbonyl group.[43,44] These IR spectra indicate the participation of the carboxyl and carbonyl groups in the complexation of CIP with Cu(II). Thus, it is inferred that the ketonic and carboxylate oxygen atoms of CIP bind directly with Cu(II).

We also optimized the structure of the Cu(II)-CIP complex by DFT calculation, and found that Cu(II) is bound to six O atoms, with two coming from the carbonyl and the carboxyl group of CIP and four from water molecules (Fig. 1). Thus, $H_2CIP^+$ (the dominant dissociation species of CIP in pH = 7.5 solution) can chelate with hydrated Cu(II) to form $[Cu(H_2CIP)(H_2O)_4]^{3+}$.

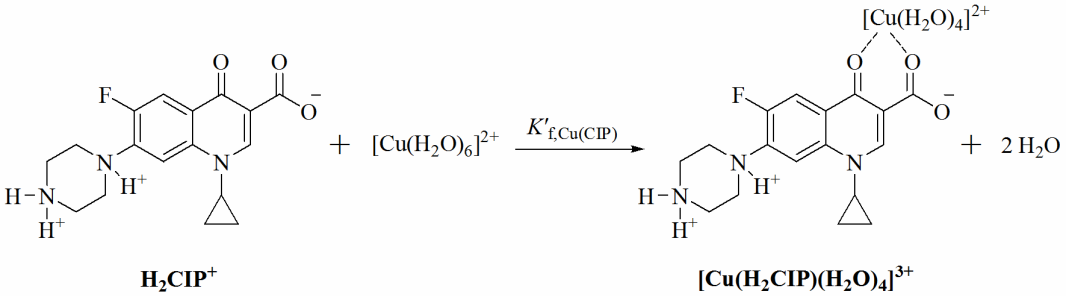


**Fig. 1** Complexing reaction between $H_2CIP^+$ and $[Cu(H_2O)_6]^{2+}$

**Effects of Cu(II) Complexation on the Apparent Photodegradation Kinetics in Aerated**

**Solutions**

In the dark control experiments, the loss of CIP [either in the presence or absence of Cu(II) and/or EDTA] was < 3%. Thus, the degradation by other processes was negligible during the photolytic experiments. Linear regression of $\ln(C_t/C_0)$ vs time ($t$) showed that the photodegradation of CIP follows pseudo-first order kinetics ($r > 0.99$, $p < 0.05$). The apparent photolytic rate constants ($k$) of CIP under different conditions are shown in Fig. 2. With the concentration of Cu(II) increasing from 0 to 20 μmol/L, the $k$ values decreased from 1.21 ± 0.03 to 0.21 ± 0.02 $h^{-1}$, indicating that Cu(II) significantly inhibits the photodegradation of $H_2CIP^+$. However, with the coexistence of Cu(II) (10 μmol/L) and EDTA (20 μmol/L), the $k$ value is similar to that in pure water. Under this condition, Cu(II) mainly chelates with EDTA (> 99.9%) instead of CIP, as $K'_{f,Cu(EDTA)}$ is about ten orders of magnitude higher than $K'_{f,Cu(CIP)}$. Additionally, the $k$ values are nearly the same for CIP dissolved in pure water and in the solution with coexistence of EDTA, indicating that EDTA does not interfere with the apparent photodegradation of $H_2CIP^+$. Thus, we found that Cu(II) affects the apparent photodegradation of $H_2CIP^+$ mainly through its complexation with $H_2CIP^+$.

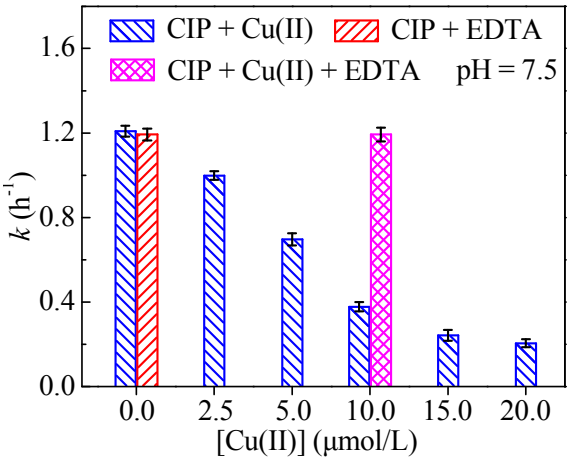


**Fig. 2** Effects of Cu(II) and EDTA on the apparent photolytic rate constants ($k$) of CIP in aerated solutions ($[CIP]_0$ = 5 μmol/L, [EDTA] = 20 μmol/L. The error bars represent the 95% confidence interval, $n$ = 3)

**Effects of Cu(II) Complexation on the Light Absorption Characteristics**

The UV-vis absorbance spectra of CIP at various Cu(II) concentrations are shown in Fig. S4. In the presence of Cu(II), the short wavelength absorption band ($\lambda_{max} \approx 275$ nm) of CIP showed a red shift with its intensity increasing, and the broad absorption band (around 310~335 nm) displayed a blue shift.

We employed DFT to calculate the molecular orbital composition for the main absorptions of $H_2CIP^+$ and $[Cu(H_2CIP)(H_2O)_4]^{3+}$ (oscillator strengths > 0.1). As shown in Table S1, the lowest-lying absorption ($\lambda$ = 322.3 nm) for $H_2CIP^+$ corresponds to the transition from the highest occupied molecular orbital (HOMO) to the lowest unoccupied molecular orbital (LUMO). For $[Cu(H_2CIP)(H_2O)_4]^{3+}$, in contrast, the lowest-lying absorption ($\lambda$ = 315.5 nm) corresponds to the transitions both from the second highest occupied molecular orbital (HOMO−1) to HOMO and from HOMO to LUMO. The difference in the light absorption between $H_2CIP^+$ and $[Cu(H_2CIP)(H_2O)_4]^{3+}$ can be further rationalized by inspection of their relevant orbital structures. As shown in Fig. S5, the lowest-lying excitation for $H_2CIP^+$ is of a $\pi,\pi^*$ nature. For $[Cu(H_2CIP)(H_2O)_4]^{3+}$, the excitation involves both charge transfer transition from the ligand to the metal and d,d transition. Thus, the Cu(II) complexation can alter the molecular orbital components of the excitation and orbital structures, which causes $[Cu(H_2CIP)(H_2O)_4]^{3+}$ to show different light absorption characteristics from $H_2CIP^+$.

**Effects of Cu(II) Complexation on the Direct Photolytic Pathways**

As shown in Fig. 2 and Fig. 3, the direct photolytic rates (determined in $N_2$-saturated solutions) of CIP with and without Cu(II) are higher than the corresponding apparent photolytic rates (determined in the aerated solutions) due to the removal of dissolved oxygen, an excited triplet quencher. The direct photolytic rate constant ($k_d$) of CIP was decreased in the presence of Cu(II), indicating that Cu(II) can significantly inhibit the direct photodegradation of $H_2CIP^+$. We identified two defluorination products (P288 and P330) formed in the direct

photodegradation of CIP (Table S2 and Fig. S6). The evolution of the products in the absence and presence of Cu(II) is depicted in Fig. 4. With the co-existence of Cu(II), the formation of P288 was slightly suppressed, and the generation of P330 was significantly inhibited. According to our previous study, P288 was generated by cleavage of the C−F bond, and P330 was formed by $OH^-$ addition.[20] Thus, the Cu(II) complexation inhibited the direct photodegradation of $H_2CIP^+$ mainly through lowering its reactivity towards $OH^-$. As the molecular structures of P288 and P330 (Fig. 4) contain carbonyl and carboxyl groups, P288 and P330 may also chelate with Cu(II), and the photodegradation of P288 and P330 could be impacted by the concomitant Cu(II) as well.

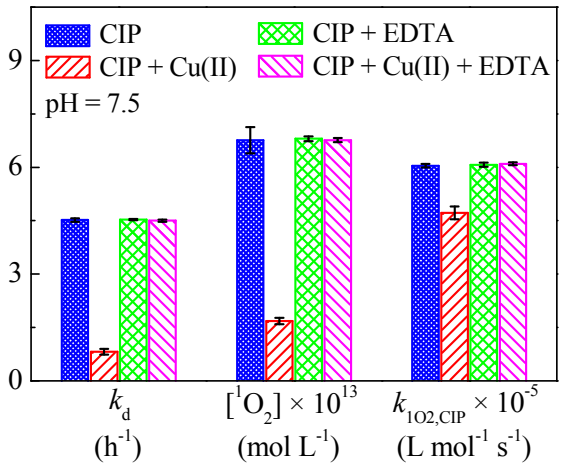


**Fig. 3** Effects of Cu(II) and EDTA on the direct photolytic rate constant ($k_d$, determined in $N_2$-saturated solutions), steady concentration of $^1O_2$ and bimolecular rate constants of CIP with $^1O_2$ (For the determination of $k_d$ and $[^1O_2]$, $[CIP]_0$ = 5 μmol/L, [Cu(II)] = $[FFA]_0$ = 10 μmol/L, [EDTA] = 20 μmol/L. For the determination of $k_{1O2,CIP}$, $[CIP]_0 = [FFA]_0$ = 20 μmol/L, [Cu(II)] = 40 μmol/L, [EDTA] = 80 μmol/L. The error bars represent the 95% confidence interval, $n$ = 3)

We further employed the DFT calculation to simulate the C−F bond cleavage and $OH^-$ addition reactions for $H_2CIP^+$ and $[Cu(H_2CIP)(H_2O)_4]^{3+}$, for which the results are detailed in

Text S3 and Table S3. The activation free energies ($\Delta G^{\ddagger}$) for the C−F bond cleavage of $H_2ClP^+$ and $[Cu(H_2ClP)(H_2O)_4]^{3+}$ are 27.3 and 32.8 kcal/mol, respectively. As shown in Fig. S7, there is no significant difference in the calculated C−F bond lengths and atomic charges on F between the two species. Thus, the Cu(II) complexation has negligible effects on the C−F bond cleavage of $H_2ClP^+$. For $OH^-$ addition, $\Delta G^{\ddagger}$ of $[Cu(H_2ClP)(H_2O)_4]^{3+}$ (10.8 kcal/mol) is about 2 times higher than that of $H_2ClP^+$ (Table S3). Since the $OH^-$ addition is a nucleophilic attack, we calculated the atomic charges on $C_{12}$ ($q_{C12}$). As shown in Fig. S8, $q_{C12}$ of $[Cu(H_2ClP)(H_2O)_4]^{3+}$ was about half of that of $H_2ClP^+$. Thus, we conclude that the lower reactivity of $[Cu(H_2ClP)(H_2O)_4]^{3+}$ with $OH^-$ is to be ascribed to the charge rearrangement of $H_2ClP^+$ caused by the complexation.

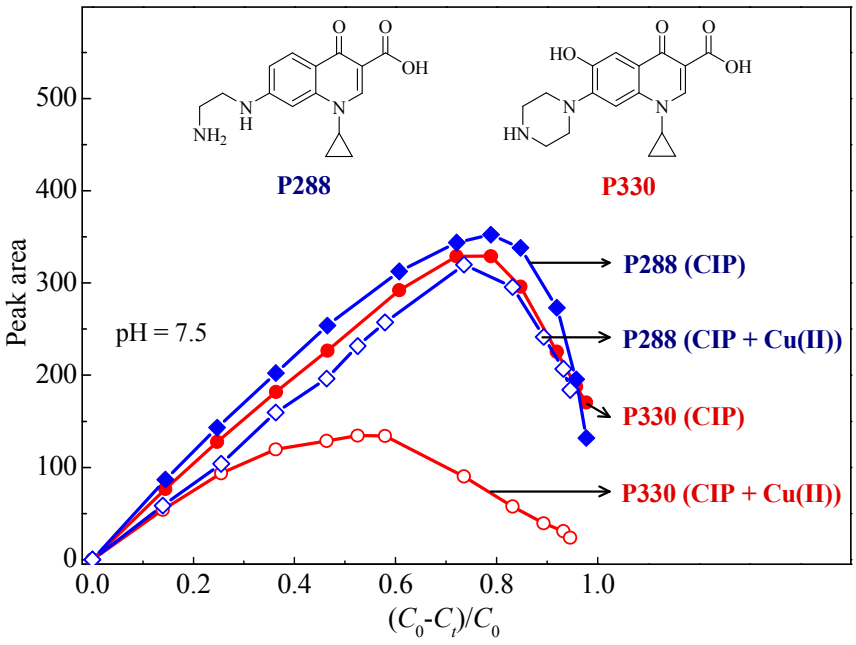


**Fig. 4** Molecular structures and evolution profiles for the photoproducts from direct photolysis (determined in $N_2$-saturated solutions) of CIP with and without Cu(II), where $[CIP]_0$ = 5 μmol/L, [Cu(II)] = 10 μmol/L, and $(C_0-C_t)/C_0$ indicates the proportion of CIP consumed at time *t*

**Effects of Cu(II) Complexation on the $^1O_2$ Reactions**

As shown in Fig. 3, with the co-existence of Cu(II), both the steady concentration of $^1O_2$ ($[^1O_2]$) and the bimolecular rate constants of CIP with $^1O_2$ ($k_{1O2,CIP}$) were lower, implying that $[Cu(H_2CIP)(H_2O)_4]^{3+}$ has a lower $^1O_2$ generation ability and weaker reactivity towards $^1O_2$. In a previous study on phototoxic potential of norfloxacin, Martinez et al. also observed that the $^1O_2$ yields were depressed in the presence of Ca(II) and Mg(II).[45] Three products (P306, P334 and P263) were identified in the $^1O_2$ oxidation reactions of CIP with and without Cu(II) (Table S2 and Fig. S6). According to the molecular structures of these products, the $^1O_2$ oxidation mainly occurs at the piperazine ring of CIP. As shown in Fig. 5, the presence of Cu(II) enhanced the production of P306, and decreased the generation of P334. Thus, the Cu(II) complexation can not only inhibit the reactivity of CIP towards $^1O_2$, but also alter the oxidation product distribution. It deserves mentioning that as the molecular structures of P306, P334 and P263 (Fig. 5) contain carbonyl and carboxyl groups, these products may also chelate with Cu(II), and the complexes may have different $^1O_2$ reactivity compared with the ligands.

According to Leach et al.[46] and Gollnick et al.[47], $^1O_2$ is an electrophile that can oxidize unsaturated C=C bonds and amino N atoms. The attack of $^1O_2$ is expected to primarily occur at molecular sites with the highest electron density. Our DFT calculation results show that for the two CIP species, the largest negative atomic charges are located at $N_{15}$ and $N_{18}$ of the piperazine ring (Table S4). Previous DFT calculation studies also indicated that the N atoms of levofloxacin and norfloxacin bear negative charges.[48,49] The calculated atomic charges imply that $N_{15}$ and $N_{18}$ are the preferred sites for attack of $^1O_2$, and the identified products also confirmed this preference. For $H_2CIP^+$, the charges on $N_{15}$ and $N_{18}$ are $-0.63e$ and $-0.61e$, respectively, indicating that $N_{15}$ and $N_{18}$ have similar reactivity towards $^1O_2$. In the case of $[Cu(H_2CIP)(H_2O)_4]^{3+}$, the charge on $N_{15}$ ($-0.68e$) is more negative than that on $N_{18}$ ($-0.58e$),

which implies that $^1O_2$ may attack $N_{15}$ more favorably than $N_{18}$. The evolution of the two products, P306 formed from the attack at $N_{15}$ and P334 formed from the attack at $N_{18}$ (Fig. 5), supports the results suggested by the atomic charges. Thus, this study also found that the Cu(II) complexation can alter the $^1O_2$ oxidation reaction pathways of CIP due to the rearrangement of atomic charges.

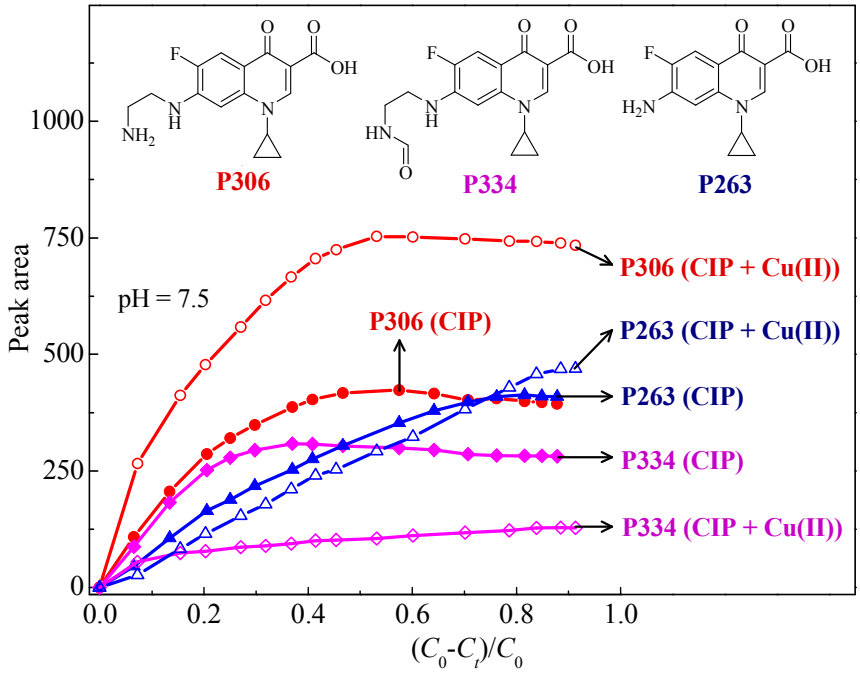


**Fig. 5** Molecular structures and evolution profiles for the $^1O_2$ photooxidation products of CIP with and without Cu(II), where $[Perinaphthenone]_0 = [CIP]_0 = 20$ μmol/L, [Cu(II)] = 40 μmol/L, and $(C_0-C_t)/C_0$ indicates the proportion of CIP consumed at time *t*

## Implications

In natural waters, Cu(II) can not only complex with CIP, but also with the concomitant dissolved organic matter (DOM).[50] According to the studies of Ahmed et al.[41] and Lofts et al.[42] on the copper-speciation in freshwaters over a wide range of metal-organic matter ratios, the concentration of free bivalent copper ion ($[Cu^{2+}]$) under equilibrium conditions is in the range of $10^{-6}$~$10^{-16}$ mol/L. As shown in Fig. 2, the *k* value in the solution with the total

concentration of Cu(II) ([Cu(II)]) = 2.5 μmol/L, where [$Cu^{2+}$] is 0.5 μmol/L and is within the range of [$Cu^{2+}$] in natural waters, is lower than that in pure water. Thus, the Cu(II) complexation can inhibit the apparent photodegradation of $H_2CIP^+$ under the environmental conditions.

This study also found that Cu(II) complexation can alter the light absorption, direct photolytic pathways, $^1O_2$ photo-generation ability, and the reactivity of $H_2CIP^+$ towards $^1O_2$. As the $^1O_2$ photo-generation ability of $H_2CIP^+$ was inhibited by the complexation, it can be inferred that the photosensitized toxicity[51] of $H_2CIP^+$ may also be altered by Cu(II) complexation. As the photolytic pathways and product distribution were also altered by the complexation, it can be assumed that the photomodified toxicity[51] of $H_2CIP^+$ may be altered too. Certainly, in addition to the photosensitized and photomodified toxicity, the toxicity of Cu(II), $H_2CIP^+$ and the photoproducts can also be impacted by the complexation. Zhang et al. investigated the toxicity of CIP and oxytetracycline to *Scenedesmus obliquus* and *Vibrio fischeri*, and found that in the presence of the transition metals Cu(II), Zn(II) and Cd(II), the formed complexes are commonly more toxic than the corresponding metals or ligands.[13] Thus, the complexation of concomitant Cu(II) can alter the environmental risk of $H_2CIP^+$. For accurate risk assessment of antibiotics in the presence of metals, it is of importance to understand the effect of metal complexation on their environmental behavior and toxicology.

According to our previous studies,[20] CIP may exhibit five dominant dissociation forms in water. The different dissociation species of CIP can chelate with different metal ions to form distinct complexes.[52] At different pH conditions, the impacts of Cu(II) on the apparent photolytic rate constants of CIP are dissimilar (Fig. S9), suggesting that the effects of Cu(II) complexation on the photodegradation of CIP in its different dissociation forms are distinct. As shown in Fig. S10 and Fig. S11, due to complexation mainly, Ca(II) and Fe(III) can also inhibit the apparent photolysis of CIP in pH = 7.5 aerated solutions. The order of inhibition

strength was Cu(II) > Fe(III) > Ca(II). Thus, it can be concluded that one specific metal ion can have different complexation effects on the photochemical behavior of different organic pollutants and their different dissociation species; and different metal ions have different impacts on the photochemical behavior of a specific organic pollutant. More studies are needed to understand the general effects of metal complexation on the photochemical behavior of organic micropollutants. Given the huge and ever-increasing number of organic pollutants,[4] it is also necessary to develop computational models that can predict the aquatic photochemical behavior of organic pollutants and their different dissociation and metal complexation forms.

## Acknowledgements

We thank Prof. Dr. Willie Peijnenburg (Leiden University) for improving the English expression and suggestions. The study was supported by the National Basic Research Program (2013CB430403) and National Natural Science Foundation (21137001, 21325729) of China.

## Notes and references

1 G.T. Ankley, B.W. Brooks, D.B. Huggett, J.P. Sumpter, *Environ. Sci. Technol.*, 2007, **41**, 8211-8217.

2 E. Gullberg, S. Cao, O.G. Berg, C. Ilback, L. Sandegren, D. Hughes, D.I. Andersson, *Plos. Pathog.*, 2011, **7**, e1002158.

3 A. Sapkota, A.R. Sapkota, M. Kucharski, J. Burke, S. McKenzie, P. Walker, R. Lawrence, *Environ. Int.*, 2008, **34**, 1215-1226.

4 R.P. Schwarzenbach, B.I. Escher, K. Fenner, T.B. Hofstetter, C.A. Johnson, U. von Gunten, B. Wehrli, *Science*, 2006, **313**, 1072-1077.

5 S.C. Zou, W.H. Xu, R.J. Zhang, J.H. Tang, Y.J. Chen, G. Zhang, *Environ. Pollut.*, 2011,

**159**, 2913-2920.

6 W. Meng, Y.W. Qin, B.H. Zheng, L. Zhang, *J. Environ. Sci.*, 2008, **20**, 814-819.

7 A. Serafin and A. Stanczak, *Russ. J. Coord. Chem.*, 2009, **35**, 81-95.

8 M.O. Schmitt and S. Schneider, *Phys. Chem. Comm.*, 2000, **3**, 42-55.

9 D.L. Ross, S.K. Elkinton, S.R. Knaub, C.M. Riley, *Int. J. Pharm.*, 1993, **93**, 131-138.

10 W.R. Chen and C.H. Huang, *Environ. Sci. Technol.*, 2009, **43**, 401-407.

11 J.J. Werner, W.A. Arnold, K. McNeill, *Environ. Sci. Technol.*, 2006, **40**, 7236-7241.

12 Z. Simon, B. Katja, U. Darko, V. Marjan, K. Albin, *J. Pharmaceut. Biomed.*, 2010, **53**, 655-659.

13 Y. Zhang, X.Y. Cai, X.M. Lang, X.L. Qiao, X.H. Li, J.W. Chen, *Environ. Pollut.*, 2012, **166**, 48-56.

14 Y. Li, J.F. Niu, W.L. Wang, *Chemosphere*, 2011, **85**, 892-897.

15 L.K. Ge, J.W. Chen, J. Lin, X.Y. Cai, *Environ. Sci. Technol.*, 2009, **43**, 3101-3107.

16 S.W. Yan and W.H. Song, *Environ. Sci.: Processes Impacts*, 2014, **16**, 697-720.

17 L.K. Ge, J.W. Chen, X.X. Wei, S.Y. Zhang, X.L. Qiao, X.Y. Cai, Q. Xie, *Environ. Sci. Technol.*, 2010, **44**, 2400-2405.

18 J.K. Challis, M.L. Hanson, K.J. Friesen, C.S. Wong, *Environ. Sci.: Processes Impacts*, 2014, **16**, 672-696.

19 D. Vione, J. Feitosa-Felizzola, C. Minero, S. Chiron, *Water Res.*, 2009, **43**, 1959-1967.

20 X.X. Wei, J.W. Chen, Q. Xie, S.Y. Zhang, L.K. Ge, X.L. Qiao, *Environ. Sci. Technol.*, 2013, **47**, 4284-4290.

21 M.C. Cuquerella, A. Belvedere, A. Catalfo, M.A. Miranda, J.C. Scaiano, G. de Guidi, *J. Photoch. Photobio. B*, 2010, **101**, 295-303.

22 U. Hubicka, J. Krzek, B. Zuromska, M. Walczak, M. Zylewski, D. Pawlowski, *Photoch. Photobio. Sci.*, 2012, **11**, 351-357.

23 M. Mella, E. Fasani, A. Albini, *Helv. Chim. Acta*, 2001, **84**, 2508-2519.

24 G.D. Christian, *Analytical Chemistry, 6th ed*, Wiley, New York, 2007.

25 F. Wilkinson, W.P. Helman, A.B. Ross, *J. Phys. Chem. Ref. Data*, 1995, **24**, 663-1021.

26 D.E. Latch, B.L. Stender, J.L. Packer, W.A. Arnold, K. McNeill, *Environ. Sci. Technol.*, 2003, **37**, 3342-3350.

27 W.R. Haag, J. Hoigne, E. Gassman, A.M. Braun, *Chemosphere*, 1984, **13**, 631-640.

28 M.J. Frisch, G.W. Trucks, H.B. Schlegel, G.E. Scuseria, M.A. Robb, J.R. Cheeseman, G. Scalmani, V. Barone, B. Mennucci, G.A. Petersson, H. Nakatsuji, M. Caricato, X. Li, H.P. Hratchian, A.F. Izmaylov, J. Bloino, G. Zheng, J.L. Sonnenberg, M. Hada, M. Ehara, K. Toyota, R. Fukuda, J. Hasegawa, M. Ishida, T. Nakajima, Y. Honda, O. Kitao, H. Nakai, T. Vreven, J.A. Montgomery, Jr., J.E. Peralta, F. Ogliaro, M. Bearpark, J.J. Heyd, E. Brothers, K.N. Kudin, V.N. Staroverov, R. Kobayashi, J. Normand, K. Raghavachari, A. Rendell, J.C. Burant, S.S. Iyengar, J. Tomasi, M. Cossi, N. Rega, J.M. Millam, M. Klene, J.E. Knox, J.B. Cross, V. Bakken, C. Adamo, J. Jaramillo, R. Gomperts, R.E. Stratmann, O. Yazyev, A.J. Austin, R. Cammi, C. Pomelli, J.W. Ochterski, R.L. Martin, K. Morokuma, V.G. Zakrzewski, G.A. Voth, P. Salvador, J.J. Dannenberg, S. Dapprich, A.D. Daniels, O. Farkas, J.B. Foresman, J.V. Ortiz, J. Cioslowski, D.J. Fox, Gaussian 09, Revision A.02; Gaussian, Inc.: Wallingford, CT (2009).

29 Y. Zhao and D.G. Truhlar, *Theor. Chem. Acc.*, 2008, **120**, 215-241.

30 P.J. Hay and W.R. Wadt, *J. Chem. Phys.*, 1985, **82**, 270-283.

31 J. Tomasi, B. Mennucci, R. Cammi, *Chem. Rev.*, 2005, **105**, 2999-3093.

32 S. Monti, S. Sortino, E. Fasani, A. Albini, *Chem.-Eur. J.*, 2001, **7**, 2185-2196.

33 A. Albini and S. Monti, *Chem. Soc. Rev.*, 2003, **32**, 238-250.

34 X.W. Yan and D. Holten, *J. Phys. Chem.-Us.*, 1988, **92**, 5982-5986.

35 M.H. Ha-Thi, N. Shafizadeh, L. Poisson, B. Soep, *J. Phys. Chem. A*, 2013, **117**,

8111-8118.

36 K. Nozaki, K. Takamori, Y. Nakatsugawa, T. Ohno, *Inorg. Chem.*, 2006, **45**, 6161-6178.

37 F. Wang and T. Ziegler, *J. Chem. Phys.*, 2005, **122**, 074109.

38 K. Fukui, *Accounts Chem. Res.*, 1981, **14**, 363-368.

39 R.S. Mulliken, *J. Chem. Phys.*, 1955, **23**, 2338-2342.

40 C. Fortin, Y. Couillard, B. Vigneault, P.G.C. Campbell, *Aquat. Geochem.*, 2010, **16**, 151-172.

41 I.A.M. Ahmed, J. Hamilton-Taylor, S. Lofts, J.C.L. Meeussen, C. Lin, H. Zhang, W. Davison, *Environ. Sci. Technol.*, 2013, **47**, 1487-1495.

42 S. Lofts and E. Tipping, *Environ. Chem.*, 2011, **8**, 501-516.

43 J. Coates, *Interpretation of infrared spectra, a practical approach*, John Wiley and Sons, New York, 2000.

44 P. Trivedi and D. Vasudevan, *Environ. Sci. Technol.*, 2007, **41**, 3153-3158.

45 L. Martinez, P. Bilski, C.F. Chignell, *Photochem. Photobiol.*, 1996, **64**, 911-917.

46 A.G. Leach and K.N. Houk, *Chem. Commun.*, 2002, 1243-1255.

47 K. Gollnick and J.H.E. Lindner, *Tetrahedron Lett.*, 1973, **14**, 1903-1906.

48 B. De Witte, H. Van Langenhove, K. Hemelsoet, K. Demeestere, P. De Wispelaere, V. Van Speybroeck, J. Dewulf, *Chemosphere*, 2009, **76**, 683-689.

49 K.A.K. Musa and L.A. Eriksson, *J. Phys. Chem. A*, 2009, **113**, 10803-10810.

50 K. Ndungu, *Environ. Sci. Technol.*, 2012, **46**, 7644-7652.

51 M. Grote, G. Schüürmann, R. Altenburger, *Environ. Sci. Technol.*, 2005, **39**, 4141-4149.

52 B. Urbaniak and Z.J. Kokot, *Anal. Chim. Acta*, 2009, **647**, 54-59.